

Measurement of non-strange D-meson production and azimuthal anisotropy in Pb–Pb collisions with ALICE at the LHC

Syaefudin Jaelani for the ALICE Collaboration

Utrecht University, Princetonplein 1, 3584 CC Utrecht, Netherlands,
syaefudin.jaelani@cern.ch

Abstract. Heavy quarks are effective probes of the properties of the QGP created in ultra-relativistic heavy-ion collisions. The ALICE Collaboration measured the non-strange D-meson production in Pb–Pb collisions at $\sqrt{s_{\text{NN}}} = 5.02$ TeV. The in-medium energy loss can be studied via the nuclear modification factor measurement. The measurement of the D-meson elliptic flow, v_2 , allows us to investigate the participation of the heavy quarks in the collective expansion of the system at low momentum and their possible thermalization in the medium. Furthermore the Event-Shape Engineering technique is used to measure D-meson elliptic flow in order to study the coupling of the charm quarks to the light quarks of the underlying medium.

Keywords: Heavy quarks, nuclear modification factor, elliptic flow

1 Introduction

Heavy quarks (i.e. charm and beauty) are effective probes of the Quark-Gluon Plasma (QGP) which is formed in ultra-relativistic heavy-ion collisions. Due to their large masses, heavy quarks are produced in hard scattering processes in the early stages of the collision before the QGP formation, which is about 0.3–1.5 fm/ c at the LHC energies [1]. Thus, they experience the full evolution of the medium and lose part of their energy interacting with the medium constituents via gluon radiation [2, 3] or collisional processes [4–6].

The in-medium energy loss can be studied by measuring the nuclear modification factor (R_{AA}). Information on the transport properties of the medium is obtained by the measurement of the azimuthal anisotropy in the momentum distribution of heavy-flavour hadrons, the elliptic flow v_2 . The measurement of the D-meson v_2 allows us to investigate the participation of low-momentum heavy quarks in the collective expansion of the system and their possible thermalization in the medium.

2 Non-strange D-meson reconstruction

In ALICE, the non-strange D mesons (D^0 , D^+ and D^{*+}) are reconstructed in the hadronic decay channels $D^0 \rightarrow K^-\pi^+$ (with branching ratio, BR, of (3.93

$\pm 0.04\%)$, $D^+ \rightarrow K^-\pi^+\pi^+$ (BR of $(9.46 \pm 0.24)\%$) and $D^{*+} \rightarrow D^0\pi^+$ (BR of $(67.7 \pm 0.5)\%$) [7], and their charge conjugates. The decay topologies are resolved via secondary vertex reconstruction thanks to the excellent performance of the Inner Tracking System. Background is reduced by applying topological selections in order to enhance the signal-to-background ratio. In addition, charged pions and kaons are identified using information from the Time Projection Chamber and the Time Of Flight detector. Finally, an invariant mass analysis is used to extract the D-meson yields. The correction for acceptance and efficiency was determined using Monte Carlo simulations based on transport code [8] which reproduces the detector response. The HIJING [9] event generator is used to simulate the underlying Pb–Pb events and D-meson signals were added using PYTHIA6 [10] event generator. The prompt yield of D mesons is obtained by subtracting the inclusive yield from beauty-hadron decays estimated based on FONLL calculations [11,12]. The V0 scintillators, which cover the pseudorapidity region $-3.7 < \eta < -1.7$ and $2.8 < \eta < 5.1$, provide centrality and event plane angle.

3 Prompt D-meson nuclear modification factor and elliptic flow

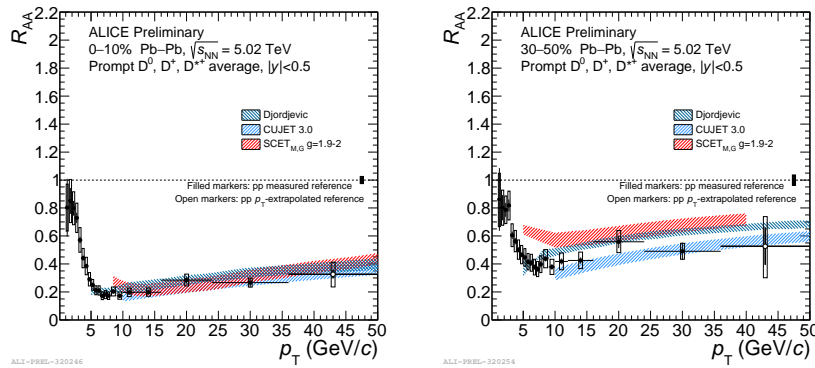


Fig. 1. Average non-strange D-meson R_{AA} in central 0-10% (left panel) and semi-central 30-50% (right panel) events in Pb–Pb collisions at $\sqrt{s_{NN}} = 5.02$ TeV compared with pQCD model predictions [13–15].

The R_{AA} of non-strange D mesons (D^0 , D^+ and D^{*+}) is measured in two centrality classes, central 0-10% and semi-central 30-50 %, in Pb–Pb collisions at $\sqrt{s_{NN}} = 5.02$ TeV. The p_T -differential cross sections of prompt D mesons in pp collisions at $\sqrt{s} = 5.02$ TeV [16] is used as reference. Figure 1 show the average non-strange D-meson R_{AA} compared to perturbative QCD model predictions in both centrality classes. The CUJET3.0 [13] and Djordjevic [14]

models which include both radiative and collisional energy loss processes, provide a fair description of the R_{AA} in both centrality classes for $p_T > 10 \text{ GeV}/c$ where radiative energy loss is expected to be the dominant interaction mechanism.

The average non-strange D-meson elliptic flow v_2 in Pb–Pb collisions at $\sqrt{s_{NN}} = 5.02 \text{ TeV}$ in the 30–50% centrality class is reported in Fig. 2 with the π^\pm , J/Ψ and charged particle v_2 in the same energy and centrality class. The v_2 of non-stange D-meson are larger than zero for $p_T > 2 \text{ GeV}/c$ in semi-central Pb–Pb collisions which indicates participation of charm quark in the collective expansion dynamics.

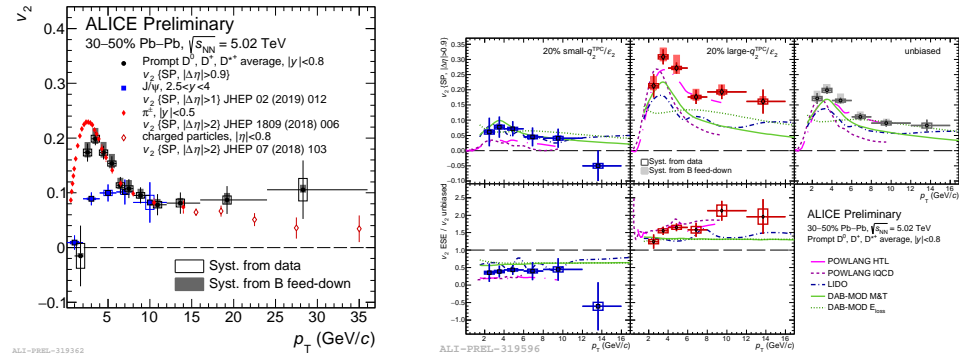


Fig. 2. Left: average non-strange D-meson v_2 in Pb–Pb collisions at $\sqrt{s_{NN}} = 5.02 \text{ TeV}$ in the 30–50% centrality class compared to the π^\pm , J/Ψ and charged particles v_2 . Right: average non-strange D-meson v_2 for the small and large q_2 , and unbiased v_2 compared with some of available models.

The Event-Shape Engineering technique was used to inverstigate the D^0 , D^+ and D^{*+} v_2 . The second-harmonic reduced flow vector, $q_2 = |Q_2|/\sqrt{M}$, can be used to quantify the eccentricity of the events, where M is the multiplicity and Q_2 is the second-harmonic flow vector. The events were divided into two groups, small- q_2 class (20% of events with smallest measured $q_2^{\text{TPC}}/q_2^{\text{V0A}}$) and large- q_2 class (20% of events with largest measured $q_2^{\text{TPC}}/q_2^{\text{V0A}}$). The average D-meson v_2 for the small- q_2 , large- q_2 and for unbiased v_2 shows in Fig. 2, on the right panel, compared with model predictions. The models are based on charm-quark transport in a hydrodynamically expanding medium. The POWLANG HTL [17] model reporoduces well the data for large- q_2 and unbiased D-meson v_2 below 12 GeV/c , while it underestimates the data for small- q_2 . The LIDO [18] and DAB-MOD [19] models provide better description of the data for small- q_2 values, while they underestimate the data for large- q_2 and unbiased D-meson v_2 .

The average R_{AA} for non-strange D mesons in the 0–10% centrality class (left) and v_2 in the 30–50% centrality class (right) are compared with Transport models in Fig. 3. Most of the models provide a fair description of the data in central events for $p_T < 10 \text{ GeV}/c$, while POWLANG [17] and BAMPS [20] in

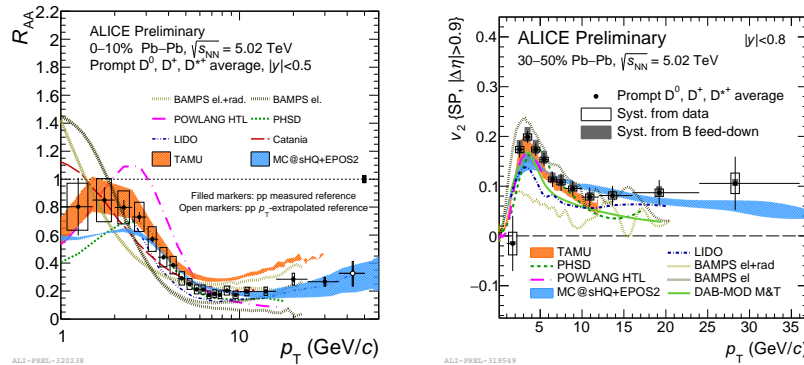


Fig. 3. Average non-strange D-meson R_{AA} in the 0-10% centrality class (left) and elliptic flow v_2 in the 30-50% centrality class (right) measured in Pb–Pb collisions at $\sqrt{s_{NN}} = 5.02$ TeV, compared with the Transport models [17, 18, 20–24].

which the interactions are only described by collisional (i.e. elastic) processes, show some tension with respect to the R_{AA} data points. The TAMU [24] model with improved space-momentum correlations between charm quarks and underlying hydro medium, describe well the D-meson v_2 for $p_T < 12$ GeV/ c . The MC@HQ+EPOS2 [21] model provides a fair description of v_2 , as does PHSD [22] and TAMU [24] for $p_T < 12$ GeV/ c , while BAMPS [20] model overestimates the maximum flow of v_2 . In addition, the LIDO [18] and DAB-MODE [19] models describe the shape of v_2 but underestimate its magnitude.

4 Conclusion

The ALICE Collaboration measured the non-strange D-meson R_{AA} and the elliptic flow v_2 in Pb–Pb collisions at $\sqrt{s_{NN}} = 5.02$ TeV. The average R_{AA} of the non-strange D-meson shows minimum values of 0.15 in the centrality class 0-10% at p_T 6.5-8 GeV/ c and 0.35 in the centrality class 30-50% at p_T 7.5-8 GeV/ c . The results of the D-meson elliptic flow v_2 are larger than zero above 2 GeV/ c in mid-central Pb–Pb collisions, which provide information of the collective expansion of the system. In addition, the Event-Shape Engineering technique for the non-strange D-meson elliptic flow v_2 was applied.

References

1. F. M. Liu and S. X. Liu, Phys. Rev. C **89**, no. 3, 034906 (2014) doi:10.1103/PhysRevC.89.034906 [arXiv:1212.6587 [nucl-th]].
2. M. Gyulassy and M. Plumer, Phys. Lett. B **243**, 432 (1990). doi:10.1016/0370-2693(90)91409-5
3. R. Baier, Y. L. Dokshitzer, A. H. Mueller, S. Peigne and D. Schiff, Nucl. Phys. B **484**, 265 (1997) doi:10.1016/S0550-3213(96)00581-0 [hep-ph/9608322].

4. M. H. Thoma and M. Gyulassy, Nucl. Phys. B **351**, 491 (1991). doi:10.1016/S0550-3213(05)80031-8
5. E. Braaten and M. H. Thoma, Phys. Rev. D **44**, 1298 (1991). doi:10.1103/PhysRevD.44.1298
6. E. Braaten and M. H. Thoma, Phys. Rev. D **44**, no. 9, R2625 (1991). doi:10.1103/PhysRevD.44.R2625
7. C. Patrignani *et al.* [Particle Data Group], Chin. Phys. C **40**, no. 10, 100001 (2016). doi:10.1088/1674-1137/40/10/100001
8. R. Brun, F. Bruyant, F. Carminati, S. Giani, M. Maire, A. McPherson, G. Patrick and L. Urban, doi:10.17181/CERN.MUHF.DMJ1
9. X. N. Wang and M. Gyulassy, Phys. Rev. D **44**, 3501 (1991). doi:10.1103/PhysRevD.44.3501
10. T. Sjostrand, S. Mrenna and P. Z. Skands, JHEP **0605**, 026 (2006) doi:10.1088/1126-6708/2006/05/026 [hep-ph/0603175].
11. M. Cacciari, M. Greco and P. Nason, JHEP **9805**, 007 (1998) doi:10.1088/1126-6708/1998/05/007 [hep-ph/9803400].
12. M. Cacciari, S. Frixione and P. Nason, JHEP **0103**, 006 (2001) doi:10.1088/1126-6708/2001/03/006 [hep-ph/0102134].
13. J. Xu, J. Liao and M. Gyulassy, JHEP **1602**, 169 (2016) doi:10.1007/JHEP02(2016)169 [arXiv:1508.00552 [hep-ph]].
14. M. Djordjevic and M. Djordjevic, Phys. Rev. C **92**, no. 2, 024918 (2015) doi:10.1103/PhysRevC.92.024918 [arXiv:1505.04316 [nucl-th]].
15. Z. B. Kang, F. Ringer and I. Vitev, JHEP **1703**, 146 (2017) doi:10.1007/JHEP03(2017)146 [arXiv:1610.02043 [hep-ph]].
16. S. Acharya *et al.* [ALICE Collaboration], Eur. Phys. J. C **79**, no. 5, 388 (2019) doi:10.1140/epjc/s10052-019-6873-6 [arXiv:1901.07979 [nucl-ex]].
17. A. Beraudo, A. De Pace, M. Monteno, M. Nardi and F. Prino, Eur. Phys. J. C **75**, no. 3, 121 (2015) doi:10.1140/epjc/s10052-015-3336-6 [arXiv:1410.6082 [hep-ph]].
18. W. Ke, Y. Xu and S. A. Bass, Phys. Rev. C **98**, no. 6, 064901 (2018) doi:10.1103/PhysRevC.98.064901 [arXiv:1806.08848 [nucl-th]].
19. C. A. G. Prado, J. Noronha-Hostler, R. Katz, A. A. P. Suaide, J. Noronha, M. G. Munhoz and M. R. Cosentino, Phys. Rev. C **96**, no. 6, 064903 (2017) doi:10.1103/PhysRevC.96.064903 [arXiv:1611.02965 [nucl-th]].
20. J. Uphoff, O. Fochler, Z. Xu and C. Greiner, J. Phys. G **42**, no. 11, 115106 (2015) doi:10.1088/0954-3899/42/11/115106 [arXiv:1408.2964 [hep-ph]].
21. M. Nahrgang, J. Aichelin, P. B. Gossiaux and K. Werner, Phys. Rev. C **89**, no. 1, 014905 (2014) doi:10.1103/PhysRevC.89.014905 [arXiv:1305.6544 [hep-ph]].
22. T. Song, H. Berrehrah, D. Cabrera, W. Cassing and E. Bratkovskaya, Phys. Rev. C **93**, no. 3, 034906 (2016) doi:10.1103/PhysRevC.93.034906 [arXiv:1512.00891 [nucl-th]].
23. S. Plumari, V. Minissale, S. K. Das, G. Coci and V. Greco, Eur. Phys. J. C **78**, no. 4, 348 (2018) doi:10.1140/epjc/s10052-018-5828-7 [arXiv:1712.00730 [hep-ph]].
24. M. He, R. J. Fries and R. Rapp, Phys. Lett. B **735**, 445 (2014) doi:10.1016/j.physletb.2014.05.050 [arXiv:1401.3817 [nucl-th]].